Supplemental Methods

Bioinformatic analysis

For 'The Cancer Genome Atlas' (TCGA) dataset Agilent-4502A microarray, data of 488 glioblastoma patients and associated clinical data were downloaded from GlioVis data portal (https://gliovis.bioinfo.cnio.es) (86). Cohorts were split into 2 groups of patients defined by the level of *SLIT2* expression, using median expression as cutoff. Overall survival (in months) was used to estimate survival distributions using the Kaplan–Meier method and the distributions were compared using the log-rank test.

For 'The Cancer Genome Atlas' (TCGA) dataset, RNAseqV2 normalized data (level 3, log2(x+1) transformed RSEM normalized count, version 2017-10-13) of 151 primary glioblastoma multiforme patients (TCGA Glioblastoma (GBM)) and associated molecular GBM subtypes and clinical data were downloaded from the cBioPortal website datapages (https://www.cbioportal.org/study/summary?id=gbm_tcga). The cohorts were split into 2 groups of patients defined by the median level of *SLIT2* expression. Overall survival (in months) was used to estimate survival distributions using the Kaplan–Meier method and the distributions were compared using the log-rank test.

Patient Samples

Frozen tumors samples were obtained from 25 patients after informed consent and approval by UZ Leuven ethical committee for the Brain-Tumor-Imm-2014 study; and tumor RNA was obtained from 104 patients of the Pitié-Salpêtrière tumor bank Onconeurotek.

RNA was purified from liquid nitrogen frozen tissue samples using RNeasy-kit (Qiagen). 0.5µg of RNA were reverse transcribed using SuperScript IV Reverse Transcriptase and Random Primers (Invitrogen) for qPCR reactions.

For the patient samples analyzed in Figure 1C/D and Supplemental Figure 1 I-N, central review histopathology of the patients classified the samples as follows:

45 patients were diagnosed with glioblastoma multiforme (GBM) grade IV, 18 patients with primary anaplastic oligodendroglioma grade III, 6 patients with primary anaplastic astrocytoma grade III, 1 patient with primary anaplastic oligoastrocytoma grade III, 16 patients with grade III mixed anaplasic gliomas, 26 patients with primary oligodendroglioma grade II, 1 patient with recurrent oligodendroglioma grade II, 4 patients with grade II astrocytomas, 9 patients with grade II mixed gliomas, 1 patient with primary xanthoastrocytoma grade II and 1 patient with primary subependymoma grade I. Associated IDH-1/2 mutation status and relevant clinical data from all the 129 patients were used in this study.

QPCR reactions

Real-time quantitative PCR (qPCR) reactions were performed in duplicate using the MyIQ real-time PCR system (Bio-Rad), with iQ SYBR Green Supermix (Bio-Rad) and QuantiTect qPCR primers (Qiagen, Supplemental Table 1). Each reaction contained 10 ng of cDNA and 250 nM forward and reverse primers. Fold changes were calculated using the comparative CT method.

Single-cell RNA sequencing analysis

We downloaded the following published datasets for single cell RNA-seq analysis from GEO: GSE138794, GSE131928, and GSE84465 (87–89). Gene expression matrices were

combined and were visualized using the Seurat v3 (90) package in R. Based on the ElbowPlot function, we chose around 43 principal components for UMAP driven visualizations. Markers for each cluster were defined from a combination of literature knowledge and the FindMarkers function in Seurat. For removal of batch effects between different datasets, we used the harmony package (91).

Murine Glioma model

Craniotomy and glioblastoma spheroid implantation were done as previously described (16). Briefly, a 5-mm circle was drilled between sutures of the skull on ketamine/xylazine anesthetized mice. A 250-µm diameter CT-2A or GL261 spheroid was injected in the cortex and sealed with a glass coverslip. For survival experiments involving PD-1 and 4-1BB inhibition, tumor cells were inoculated as cell suspension in the mice striatum instead as cortical spheroids as previously described (60). Following intramuscular administration of analgesic (buprenorphine 1 mg/kg), mice were placed in a heated cage until full recovery.

For Temozolomide (Sigma) treatment, mice were injected intraperitoneally with 40mg/kg in 0.2 mL of PBS at days 7, 11, 15 and 19 after tumor implantation. For anti-PD1 (clone RMP1-14, BioXCell) and anti-4-1BB (clone LOB12.3, BioXCell) treatment, glioma-bearing mice were injected intraperitoneally with 0.2 mg of antibodies on days 7, 9, 11 and 13 after tumor implantation.

For Robo1Fc (R&D Systems) treatment, 1-week growth glioma-bearing mice were injected intravenously with 2.5 mg/kg of Robo1Fc or human control IgG1 Fc fragment at days 7, 9, 11, 13 and 15 after tumor implantation. For this experiment, 6 different series of mice were implanted and treated: 2 for tumor volume measurement and histological analysis and 4 for survival analysis.

At the defined time points, blood samples were obtained by retro-orbital bleeding with EDTA-coated capillaries and complete blood cell counts were obtained with a HemaVet (Drew Scientific). 21 or 23 days after tumor implantation, anesthetized mice were transcardially perfused with 2% PFA solution. The mouse brain was harvested and fixed overnight in 4% PFA at 4°C. For immunohistochemistry, brains were washed with PBS and sectioned with a vibratome (200um-400µm sections). Tumor volume was measured on serial 400µm sections of the whole tumor under a stereo-microscope using Leica software according to Cavalieri's principle.

Slit2 shRNA knockdown and overexpression

CT-2A and GL261 glioma cell lines were infected with Slit2 mouse shRNA lentiviral particles (Locus ID 20563, Origene TL511128V) in accordance with the manufacturer's instructions. After infection, cells were polyclonally selected by Puromycin and GFP^+ cells were sorted by FACS. Slit2 knockdown was verified by qPCR and Western Blot analysis, and cells were implanted after a maximum of 5 passages. For Slit2 re-expression, shSlit2 CT-2A cells were infected with SLIT2 (NM_004787) Human Tagged ORF Clone Lentiviral Particle (Origene) in accordance with manufacturer's instructions. Cells were implanted after a maximum of 3 passages.

FDG PET-CT Imaging

Mice were fasted overnight with free access to water. Mice were anesthetized with isoflurane, weighed and glycemia was measured in blood drawn from the caudal ventral artery using an Accu-Chek® Aviva Nano A (Accu-Chek, France). A 26G needle catheter (Fischer Scientific, France) connected to a 5cm polyethylene tubing (Tygon Microbore Tubing, 0.010" x 0.030"OD; Fisher Scientific, France) was inserted in the caudal vein for

radiotracer injection. 9.2±1.5 MBq of 2'-deoxy-2'-[18F]fluoro-D-glucose (FDG; Advanced Applied Applications, France) in 0.2mL saline was injected via the catheter. Mice were left on a warming pad for 30 min and then installed into the PET-CT dedicated bed. Respiration and body temperature were registered. Body temperature was maintained at 34±2 °C and anesthesia was controlled on the breathing rate throughout the entire PET-CT examination. CT was acquired in a PET-CT scanner (nanoScan PET-CT; Mediso Medical Imaging Systems, Hungary) using the following acquisition parameters: semi-circular mode, 50kV tension, 720 projections full scan, 300ms per projection, binning 1:4. CT projections were reconstructed by filtered retro-projection (filter: Cosine; Cutoff: 100%) using the software Nucline 3.00.010.0000 (Mediso Medical Imaging Systems, Hungary). 55 min post tracer injection, PET data were collected for 10 min in list mode and binned using a 5ns time window, with a 400-600keV energy window and a 1:5 coincidence mode. Data were reconstructed using the Tera-Tomo reconstruction engine (3D-OSEM based manufactured customized algorithm) with expectation maximization iterations, scatter and attenuation correction. Volumes-of-interest (VOI) were delineated on the tumor and the contralateral brain on PET/CT fusion slices using the PMOD software package (PMOD Technologies Ltd, Zürich, Switzerland). Total FDG uptake was estimated as the product from the volume by the mean uptake of the segmented region.

Patient-derived GBM xenograft model (PDX)

N15-0460 patient-derived cell line (PDCL) was established by Gliotex team from GBM tissue sample that was provided by the neuropathology laboratory of Pitie-Salpetriere University Hospital, and obtained as part of routine resections from patients under their informed consent (ethical approval number AC-2013-1962). The parental tumor was

IDH-WT and MGMT methylated. Cells are cultivated in DMEM/F12 supplemented with B27, EGF (20 ng/ml), FGF (20 ng/ml), penicillin/streptomycin 1% and plasmocin 0.2%, and dissociated with Accutase. Cells were transduced with luciferase/mkate2 lentiviral particles (in-house produced) at MOI of 3 then shRNA-GFP lentiviral particles (SLIT2, Locus ID 9353, Origene TL309262V) at MOI of 3. After infection, cells were polyclonally selected by Puromycin and $mKate^+$ and GFP^+ cells were sorted by FACS (BioRad S3e Cell Sorter).

For intracranial xenografts, 1.4 x 10^5 cells were injected in 2 µL of HBSS in Hsd:Athymic Nude-Foxn1nu mice (Envigo) by stereotaxic injection at Bregma AP : +0.1 ; ML : -0.15 ; DV : -0.25 under isoflurane anesthesia (protocol #17503 2018111214011311 v5).

Tumor growth was monitored every 15 days by bioluminescence imaging following 100µL luciferin subcutaneous injection at 30mg/mL, and image acquisition with IVIS® Spectrum *in vivo* imaging system (Perkin Elmer). The development of tumors (Tumor take) was evaluated by determining the day when bioluminescence signal doubled compared to the first bioluminescence measured 8 days post-graft.

In vitro spheroid formation and invasion assays

For spheroid formation, 1,000 N15-0460 shCTRL or shSLIT2 cells were plated in non-adherent 96 well plates for 48hs and then imaged by fluorescence using a standard FITC filter to detect endogenous GFP. For invasion assays, spheroids were then resuspended in fibrinogen solution (2.5 mg/ml fibrinogen (Sigma) in DMEM/F12 supplemented with B27, EGF (20 ng/ml), FGF (20 ng/ml) and 50 mg/ml aprotinin (Sigma)) and clotted with 1 U thrombin (Sigma-Aldrich) for 20 min at 37 °C. Cultures were topped with medium and incubated at 37 °C, 5% CO2. After 1 and 2 days, cultures were imaged by fluorescence using a standard FITC filter.

Extraction of tumor-associated macrophages, lymphocytes and endothelial cells and qPCR analysis

Ketamine/Xylazine anaesthetized tumor-bearing mice were transcardially perfused with 30 ml of ice-cold PBS. Tumors were harvested and incubated with DMEM containing 2.5 mg/ml collagenase D, and 5 U/ml DNase I for 20 min at 37°C. The digested tissue was passed through a 40µm nylon cell strainer (Falcon) and red blood cells were lysed (Red Blood Cells Lysis buffer, Merck).

After blocking with mouse FcR Blocking Reagent (MACS Miltenyi Biotec) cells were stained with the following monoclonal antibodies: anti-CD45 BUV 805 (Clone 30-F11, BD), anti-CD11b BV450 (Clone M1/70, BD), anti-CD31 PE/CF594 (Clone 390, BD), and anti-CD3 BUV395 (Clone 145-2C11, BD), anti-CD4 PE (Clone GK1.5, BD) and anti-CD8 PerCP/Cy5.5 (Clone 53-6.7, BD) antibodies. TAMs ($CD45^+CD11b^+CD3^-$), TALs ($CD45^+CD11b^-CD3^+$, either $CD4^+$ or $CD8^+$), endothelial cells ($CD45^-CD31^+$) and tumor cells ($CD45^-GFP^+$) were sorted on a BD FACS Aria II. Cell viability after FACS analysis was determined using eBioscience Fixable Viability Die eFluor 780 (Invitrogen) and found to be >90%. The cells were then shock-frozen in liquid nitrogen and stored at -80°C until further use.

Total RNA was isolated using the NucleoSpin RNA XS kit from Macherey-Nagel. For protein extraction, frozen cells were resuspended in RIPA Buffer with protease and phosphatase inhibitors and sonicated 3x for 15 seconds each time. Protein concentration was determined by the BCA method and ELISAs were performed according to the manufacturer's instructions (Mouse VEGF, IL-10 and IFNγ DuoSet ELISA, R&D Systems).

Flow-cytometric staining of tumor-infiltrating immune cells

Day 21 CT-2A shCTRL and shSlit2 tumors were harvested and dissociated as described. Single cell suspensions were incubated with anti-CD45 Alexa Fluor 594 (Clone 30-F11, R&D Systems) or BUV805 (Clone 30-F11, BD), anti-CD11b BV450 (Clone M1/70, BD), anti-Ly6G PerCP/Cy5.5 (Clone 1A8, BD), anti-Ly6C APC/Cy7 (Clone AL-21, BD), anti-F4/80 PE (Clone BM8, BD), anti-CD11c (Clone N418, APC), anti-MHCII PE/Cy7 (Clone M5/114.15.2, Biolegend), anti-MRC1 BV711 (Clone C068C2, Biolegend), anti-CD3 PE/Cy5 (Clone 145-2C11, Biolegend), anti-CD19 PE/Texas Red (Clone 1D3, BD), anti-CD4 PE (Clone GK1.5, Biolegend), and anti-CD8 PerCP/Cy5.5 (Clone 53-6.7, Biolegend). As a control, cells were stained with the appropriate isotype control. Data acquisition was performed on BD LSRFortessa X20 and analysis was performed with FlowJo_V10.

Cell lines

RAW264.7 mouse macrophages, CT-2A and GL261 glioma cells were cultured in DMEM Gluta-MAX (Gibco) supplemented with 10% FBS (Gibco), 1% penicillin/streptomycin (Gibco) until a maximum of 10 passages. Glioma spheroids were obtained by seeding the glioma cells for 48 h on non-adherent culture dishes.

Cell Growth Determination

Cell viability was determined using the Cell Growth Determination Kit, MTT based (Sigma) according to manufacturer's instructions. Briefly, 20.000 cells were plated in 24 well plates and grown in normal supplemented medium over 3 days, for determination of their growth curve. After each 24-hour period, cells were incubated with 10% MTT solution for 3 hours, then MTT formazan crystals were dissolved and absorbance was

spectrophotometrically measure at 570 nm. Background absorbance measured at 690 nm was subtracted to the first value.

For TMZ sensitivity test, cells were treated for 24 hours with increasing concentrations of TMZ in serum-free medium. The same procedure was performed on untreated cells, and values were normalized and expressed in comparison to untreated cells.

Vessel perfusion and permeability assay

Glioma-bearing mice from 3 weeks growth were anesthetized and injected intravenously with 100 µL of Alexa Fluor 647 labeled 10,000 MW dextran (Life Technologies). Blood vessel perfusion was visualized in vivo using the live imaging settings.

For Miles assay, glioma-bearing mice were anesthetized and injected intravenously with 100 µL 1% Evan's blue solution (Sigma). Thirty minutes after injection, mice were sacrificed and transcardially perfused with 2% PFA solution. Dissected tumors were weighed and incubated in formamide solution at 56°C overnight to extract the dye. The absorbance of the solution was measured with a spectrophotometer at 620 nm. Five mice per group were analyzed. Data are expressed as fold change compared to shCTRL glioma growth with tumor weight normalization.

MRI

Magnetic resonance imaging (MRI) was performed 21 days after tumor implantation in mice under Isofluorane anesthesia (2 to 2.5% mixed in ambient air) in a 4.7-T magnetic resonance scanner (Bruker BioSpec 47/40USR). Brain images were obtained using a Fast-Spin-Echo (FSE) T2 weighted (TE/TR: 15/2000 ms; matrix: 128×128; slice thickness: 1 mm; with no gap; 12 averages) and a Spin-Echo (SE) T1 weighted (TE/TR: 15/250 ms; matrix: 128x128; slice thickness: 1 mm; with no gap; 12 averages) sequences

in axial and coronal planes. T1 weighted images were acquired before and T2 weighted images after intraperitoneal injection of gadoteric acid (200uL, 0.01mmol/mL, 0.05 M/Kg).

Immunofluorescence staining

Vibratome sections of tumors injected in ROSA^{mTmG} reporter mice were blocked and permeabilized in TNBT buffer (0.1 M Tris pH 7.4; NaCl 150 mM; 0.5% blocking reagent from Perkin Elmer, 0.5% Triton X-100) overnight at 4ºC. Tissues were then incubated with primary antibodies anti-F4/80 (Clone BM8, Life Technologies, 1:100), anti-MRC1 (AF2535, R&D Systems, 1:100), anti-CD3 (Clone 17A2, R&D Systems, 1:100), anti-MHCII (Clone M5/114.15.2, Thermo Scientific, 1:100), anti-Glut1 (07-1401, Millipore, 1:200), anti-Iba1 (019-19741, Wako, 1:200), anti-pH2AX (8718, Cell Signaling, 1:100) diluted in TNBT overnight at 4ºC, washed in TNT buffer (0.1 M Tris pH 7.4; NaCl 150 mM; 0.5% Triton X-100) at least 7 times and incubated with appropriate Alexa Fluor 647 conjugated antibody (Life Technologies, 1:400) diluted in TNBT overnight at 4ºC. Samples were then washed at least 7 times in TNT and mounted on slices in fluorescent mounting medium (Dako). Images were acquired using a Leica SP8 inverted confocal microscope.

Soluble Flt-1 binding assay

For detection of VEGF expression, vibratome sections were blocked and permeabilized in TNBT overnight at 4ºC. Tissues were then incubated with 1µg/ml recombinant mouse soluble Flt-1 FC chimera (321-FL-050, R&D Systems) diluted in TNBT for 2.5 h at room temperature. Samples were rinsed three times in TNT and subjected to 4% PFA fixation for 3 min. Samples were washed at least 7 times in TNT and incubated in Alexa Fluor

647 coupled anti-human IgG secondary antibodies (Life Technologies, 1:200) diluted in TNBT overnight at 4°C. Tissues were washed at least 7 times and mounted on slides in fluorescent mounting medium (Dako). Images were acquired using a Leica SP8 inverted confocal microscope.

Flow-cytometric analysis of tumor-antigen in lymph node immune cells

Deep cervical and mandibular lymph nodes (DCLN and MLN) were dissected from tumor bearing mice 21 days after injection of CT-2A BFP or CT-2A GFP tumor spheroids. The 2 DCLNs and 6 MLNs of each mice were pooled for analysis. LNs were digested for 30 minutes in 1mg/mL Collagenase I diluted in DMEM at 37ºC and after RBC lysis, single cell suspensions were prepared by filtering dissociated tissue on 40uM nylon cell strainers. Single cell suspensions were incubated with anti-CD45 APC or BUV805 (Clone 30-F11, BD), anti-CD11b BV650 or BV450 (Clone M1/70, BD) antibodies. As a control, cells were stained with the appropriate isotype control. Data acquisition was performed on the BD LSRFortessa X20 and analysis was performed with FlowJo_V10.

Primary cell cultures

Bone-marrow derived macrophages (BMDMs) were isolated from C57BL/6 mice by flushing the femur and tibia with PBS. The bone marrow cells were resuspended in DMEM GlutaMax (Gibco) containing 1% Pen/Strep (Gibco), 20% FBS (Gibco) and 100 ng/mL M-CSF (R&D Systems). Cells were incubated for 2 days at 37 °C and 5% CO2 in non-treated bacterial dishes for adhesion of bone-marrow resident macrophages, and then changed for treated plastic dishes and culture for 6 days with medium change every 2 days. Before experiments, cells were starved in serum- and CSF-free medium overnight. For PI3Kγ inhibition experiments, cells were pre-treated with 1uM IPI-549 for

30 minutes as previously described (1) and then treatments were performed as described for all other experiments.

Microglial cells were obtained as described previously (2, 3). Peritoneal macrophages (PMs) were isolated from peritoneal lavage as previously described (4).

Slit2 ELISA

Slit2 concentrations in mice serum were determined by the sandwich ELISA method with the DuoSet ELISA Ancillary Reagent Kit 2 (R&D Systems) according to the manufacturer's instructions, using serum samples obtained either from healthy mice or from tumor-bearing mice. Rat anti-Human/Mice Slit2 monoclonal antibody (Clone 710305, R&D Systems) was used as capture antibody at a concentration of 1ug/mL and sheep anti-mouse Slit2 polyclonal antibody (AF5444, R&D Systems) was used as detection antibody at a concentration of 400ng/mL HRP-linked anti-sheep secondary antibodies (1:1000) were used for revelation.

siRNA transfection

Robo1, Robo2 and control siRNAs were purchased from Origene. We transfected RAW 264.7 macrophages with 10nM final siRNA concentration using siTran1.0 transfection reagent (Origene), according to the manufacturer's instructions. Cells were used for experiments 72 h after transfection. For qPCR experiments, RNAs were purified using RNeasy-kit (Qiagen). 500 or 750 ng of RNA were reverse transcribed using SuperScript II Reverse Transcriptase and Random Primers (Invitrogen). Quantitative PCR were assayed as described for patient samples.

For adenoviral Robo1 rescue, we used previously described methods (28, 31).

Transwell Migration Assay

For chemotactic migration assays with 8.0μm Polycarbonate Membrane Transwell inserts (Corning Inc), 20.000 primary cells were plated in 125 μL of serum-free DMEM medium on the top chambers. When stated, 1.000ng/mL of rmSlit2 was also added to the top chambers. Then, bottom chambers were filled with 500 μL of serum-free DMEM with chemoattractants (R&D Systems). Cells were cultured overnight at 37°C and 5% CO_2, then incubated for 30 minutes with Calcein AM (Invitrogen) to stain live cells. Then the wells were washed and 10 pictures per well were acquired at 10x magnification using a Leica DMIRB inverted epifluorescence microscope. Migrated cells per field were counted using ImageJ software.

For Transwell migration assay in direction to tumor cells, 30.000 tumor cells were plated in the bottom chamber and starved in 500uL of serum-free media for 8 hours before plating cells on the top chamber.

Western blot analysis

Cells were lysed in RIPA lysis buffer including phosphatase and protease inhibitors (Invitrogen). Equal amounts of proteins were separated on 4–15% Criterion precast gel (Bio-rad) and transferred on nitrocellulose membrane with Transblot Turbo (Bio-rad). Then membranes were blocked in 5% non-fat milk in TBS-T for 30 minutes at room temperature and incubated with primary antibodies against Robo1 (Clone 770506, R&D Systems, 1:500), Robo2 (AF7118, R&D Systems, 1:500), Actin (Clone AC-74, Sigma, 1:4000), anti-phospo p44/42 MAP kinase (phospho-ERK, 4370, Cell Signaling, 1:1000), anti-p44/42 MAP kinase (total ERK, 9102, Cell Signaling, 1:1000), anti-pAkt Ser473 (4058, Cell Signaling, 1:1000), anti-Akt (9272, Cell Signaling, 1:1000), anti-pPLCγ Ser 1248 (4510, Cell Signaling, 1:1000), anti-PLCγ (2822, Cell Signaling, 1:1000) overnight

at 4°C under agitation. After washing with TBS-T membranes were incubated with proper HRP-conjugated secondary antibodies for 3 hours at room temperature under agitation. Western blots were developed with chemiluminescence HRP substrate (Bio-rad) on a Luminescent image analyser, ChemiDoc XRS+ (Bio-rad).

Immunoprecipitation

After Slit2 treatments for 15 minutes, BMDMs were lysed using NP40 lysis buffer (Boston bioproducts, BP-119X) supplemented with protease and phosphatase inhibitor cocktails (Roche, 11836170001 and 4906845001). Protein concentrations were quantified by BCA assay (Thermo Scientific, 23225) according to the manufacturer's instructions. 300ug of protein were diluted in 1ml of NP40 buffer containing protease and phosphatase inhibitors for each condition. In the meantime, protein A/G magnetic beads (Thermo fischer, 88802) were washed 5x 10min with NP40 buffer. Protein lysates were incubated for 2 hours at 4°C under gentle rotation with 10ug of PI3Kγ antibodies (5405, Cell Signaling Tecnologies). Then, 50ul of A/G magnetic beads were added to each protein lysate for 2 hours at 4°C under gentle rotation. Beads were then isolated using magnetic separator (Invitrogen) and washed 5 x with NP40 buffer. After the last wash, supernatants were removed and beads were resuspended in 40ul of Laemmli buffer (Bio-Rad, 1610747), boiled at 95°C for 5min and loaded onto 4-15% gradient gels. Western blotting was performed as described above.

GFP$^+$ macrophage isolation

We collected mouse femoral bone-marrows (BMs) before the sacrifice of tumor-bearing mice as previously described for BMDM cultures. In the meantime, rabbit anti-GFP antibodies (A-21311, Invitrogen) were incubated with sheep anti-rabbit IgG magnetic

dynabeads (Invitrogen) in a solution of sterile PBS 0.1%BSA (120ul of beads, 24ul of antibodies in 12ml PBS 0.1%BSA). Solutions were place under gentle rotation at room temperature for 2hours to allow proper coupling of antibodies and beads. Coupled beads were next isolated using a magnetic separator and incubated in the resuspended BMs for 30min. After 5 washes with PBS 0.1%BSA, beads were separated using magnetic separator and RNA was extracted as previously described using RNeasy-kit (Qiagen). RNA samples were and reverse transcribed using SuperScript IV RT (Invitrogen) for gene-deletion verification by qPCR.

CD3+ T cell depletion

For T cell depletion from the TME, 7-day glioma-bearing mice were injected intravenously with 0.2 mg of anti-CD3 145-2C11 monoclonal antibody (BioXCell) every 3 days and analyzed at 23 days of tumor growth.

Supplemental References

1. Kaneda MM et al. PI3Kγ 3 is a molecular switch that controls immune suppression. *Nature* 2016;539(7629). doi:10.1038/nature19834

2. Lima FRS et al. Regulation of microglial development: A novel role for thyroid hormone. *J. Neurosci.* 2001;21(6). doi:10.1523/jneurosci.21-06-02028.2001

3. do Amaral RF et al. Microglial lysophosphatidic acid promotes glioblastoma proliferation and migration via LPA1 receptor. *J. Neurochem.* [published online ahead of print: 2020]; doi:10.1111/jnc.15097

4. Pontes B et al. Membrane Elastic Properties and Cell Function. *PLoS One* 2013;8(7). doi:10.1371/journal.pone.0067708

Supplemental Figures

Supplemental Figure 1

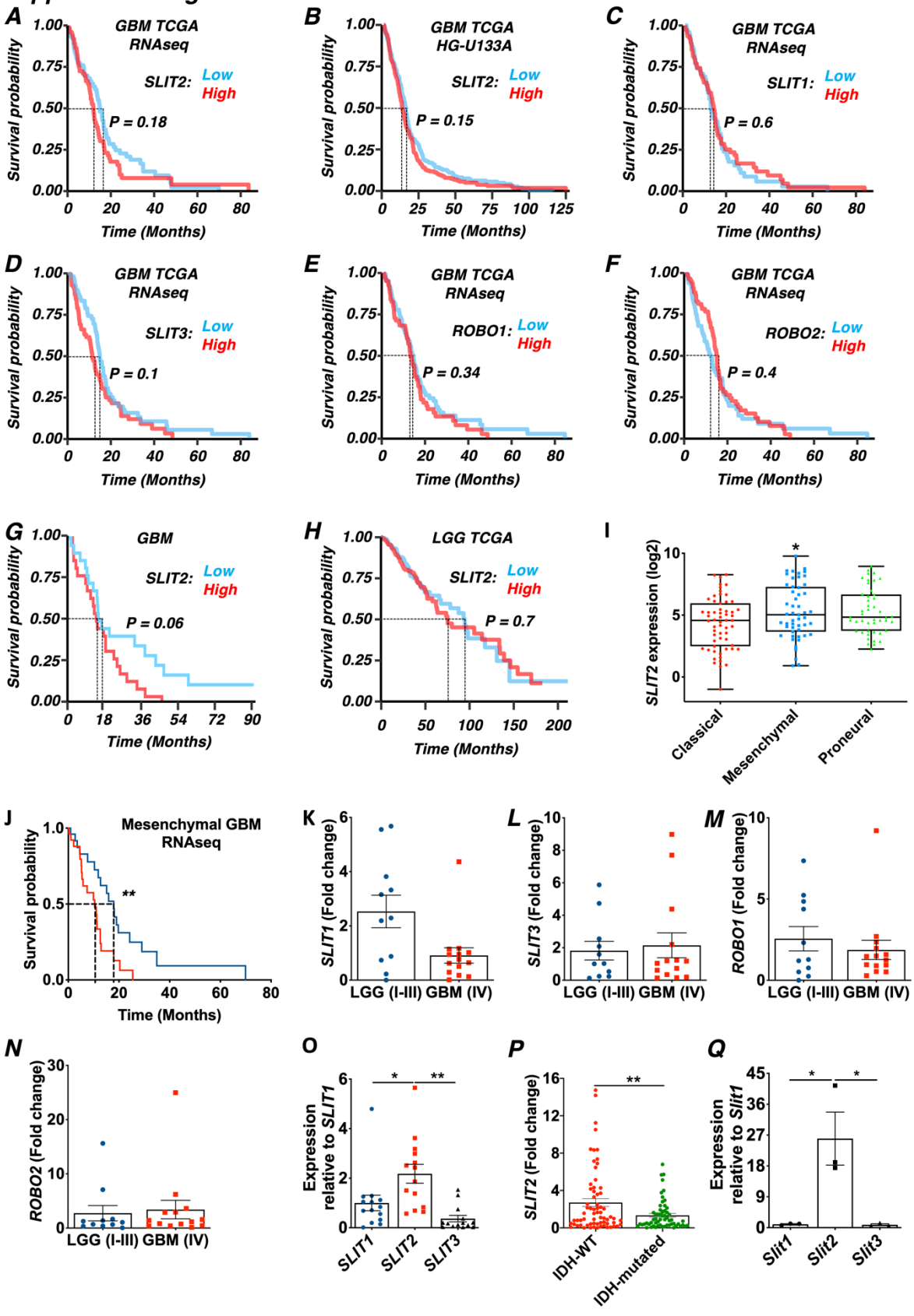

Supplemental Figure 1. Impact of Slit2 on glioma patient survival.

A. *In silico* analysis of TCGA glioblastoma RNAseq patient dataset (*n* = 75 high and 76 low Slit2 expressing patients; O.S., 12.6 months for high expression and 14.9 months for low expression, log-rank test). **B.** *In silico* analysis of TCGA glioblastoma HG-U133A patient dataset (*n* = 262 high and 263 low Slit2 expressing patients; O.S., 11.8 months for high expression and 13.6 months for low expression, log-rank test).**C-F.** *In silico* analysis of TCGA glioblastoma RNAseq patient dataset demonstrating that expression of *SLIT1* (**C**), *SLIT3* (**D**), *ROBO1* (**E**) or *ROBO2* (**F**) do not affect patient survival. **G.** Survival analysis of GBM patients from (**Figure 1C**) grouped by their levels of *SLIT2* expression (*n* = 22 high and 23 low Slit2 expressing patients; O.S., 15.2 months for high expression and 16.5 months for low expression, log-rank test). **H.** *In silico* analysis of TCGA LGG patient dataset (*n* = 255 high and 255 low Slit2 expressing patients; O.S., 75 months for high expression and 94.5 months for low expression, log-rank test). **I.** *In silico* analysis of TCGA glioblastoma RNAseq patient dataset demonstrating *SLIT2* expression in different GBM molecular subtypes (*n* = 59 classical, 51 mesenchymal and 46 proneural tumors; One-Way ANOVA). **J.** *In silico* analysis of TCGA glioblastoma RNAseq patient dataset demonstrating that *SLIT2* expression is significantly associated with decreased patient survival in mesenchymal GBM patients (*n* = 26 high and 25 low *SLIT2* expressing patients; O.S., 10.4 months for high expression and 17.9 months for low expression, log-rank test). **K-N.** qPCR expression of *SLIT1* (**K)**, *SLIT3* (**L**), *ROBO1* (**M**) and *ROBO2* (**N**) in glioma patient samples (GBM, *n* = 45; LGG, *n* = 84; Student's t test). **O**. qPCR comparison of *SLIT1*, *SLIT2* and *SLIT3* expression in GBM patient samples (Grade IV, *n* = 14 patients; One-Way ANOVA). **P.** *SLIT2* qPCR expression in all glioma patient samples from (**Figure 1C**) classified by their IDH-1/2 status (IDH-WT, *n* = 67; IDH-mutated, *n* = 59; Student's t test). **Q.** qPCR comparison of *Slit1, Slit2* and *Slit3* expression

404 in CT-2A tumors (n = 3 independent tumors, One-Way ANOVA). Data are presented as

405 mean ± s.e.m. * $P < 0.05$, ** $P < 0.01$, *** $P < 0.001$.

406

Supplemental Figure 2

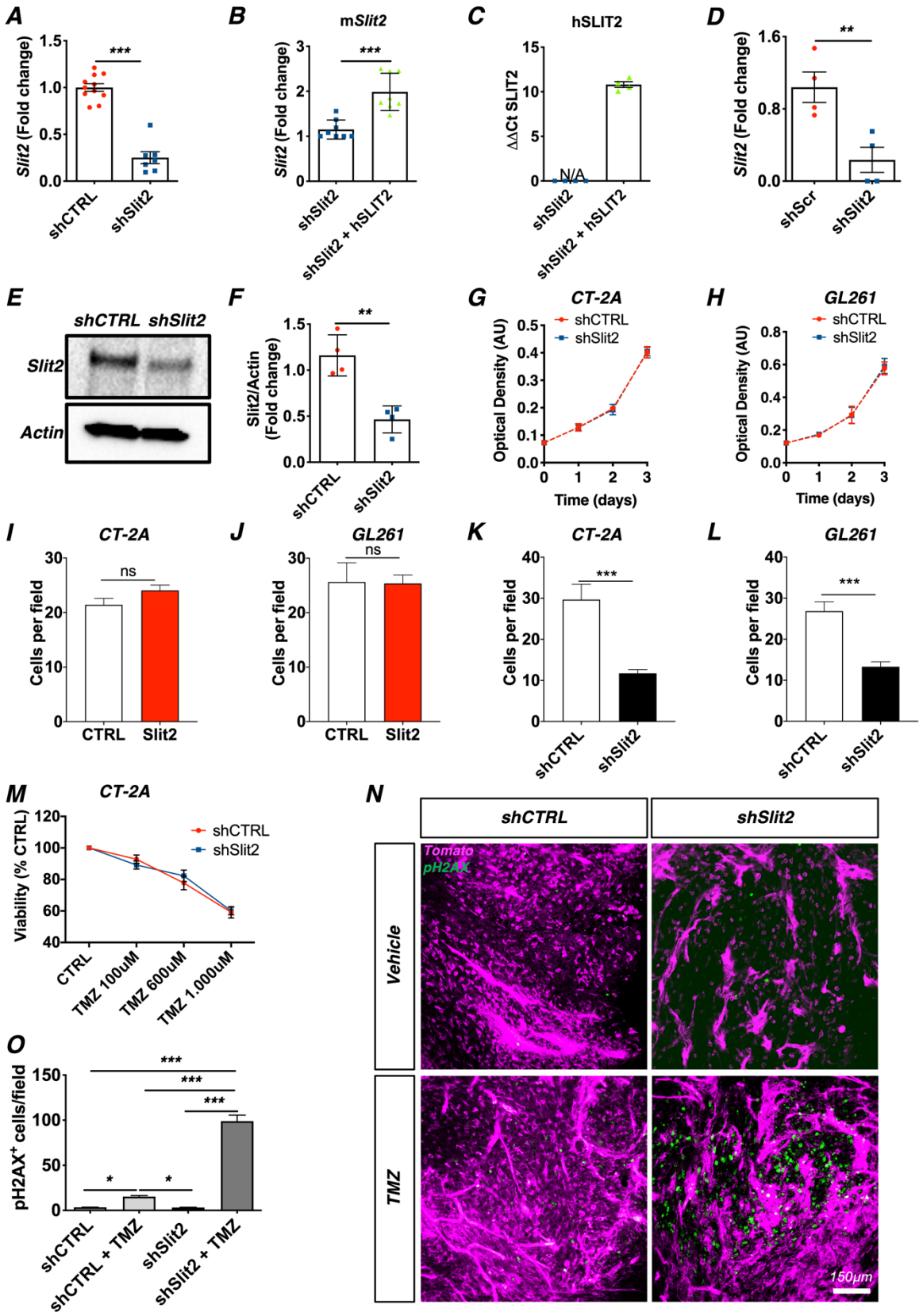

Supplemental Figure 2. Slit2 silencing does not change tumor cell proliferation or sensitivity to TMZ *in vitro*, but increases TMZ-induced tumor cell death *in vivo*.

A. *Slit2* qPCR expression in CT-2A shSlit2 and shCTRL (n = 10 shCTRL and n = 7 shSlit, Student's t-test). **B-C.** qPCR analysis of murine (**B**, n = 8) and human (**C**, n = 4) Slit2 expression in cells infected with a human SLIT2 construct (Mann-Whitney U test). **D-F.** qPCR analysis **(D),** western blot analysis **(E)** and protein quantification **(F)** of shRNA Slit2 silencing in GL261 cells (n = 4, Mann-Whitney U test). **G-H.** Kinetics of shCTRL and shSlit2 treated CT-2A **(G)** and GL261 **(H)** glioma cell growth over 72 hours in complete medium (n = 3, multiple comparison linear regression). **I-J.** Transwell assay quantification of CT-2A (**I**) and GL261 (**J**) cells migration towards a Slit2 gradient (n = 4, Mann-Whitney U test). **K-L.** Transwell assay quantification of CT-2A (**K**) and GL261 (**L**) shCTRL or shSlit2 cells invasion towards a serum gradient (n = 4, Mann-Whitney U test). **M.** *In vitro* shCTRL and shSlit2 treated CT-2A glioma cell response to TMZ treatment (n = 4, One-way ANOVA). **N.** Phospho-H2AX (pH2AX) immunostainings (green) on 23 days tumor sections of CT-2A shCTRL and shSlit2 mice treated or not with TMZ in order to evaluate double-stranded DNA breaks ($pH2AX^+$, green) in response to TMZ treatment. **O.** Quantification of **(N)** (n = 4 mice per group, 5 fields per tumor, One-way ANOVA). Data are presented as mean ± s.e.m. * $P < 0.05$, ** $P < 0.01$, *** $P < 0.001$.

Supplemental Figure 3

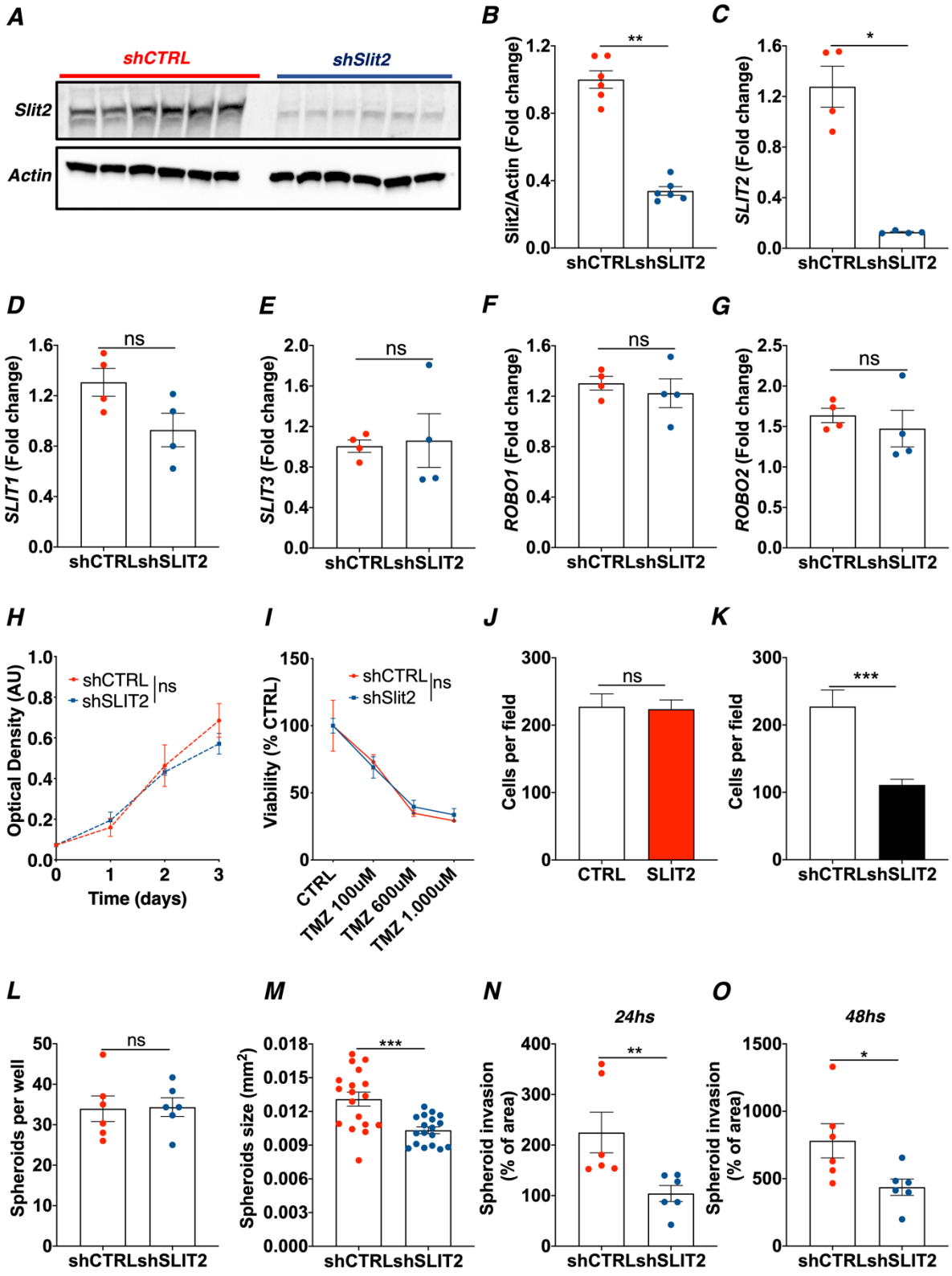

433

Supplemental Figure 3. Slit2 silencing reduces invasion of Patient-derived GBM cells.

A-C. Western blot analysis **(A)**, protein quantification **(B)** and qPCR analysis **(C)** of shRNA *SLIT2* silencing in N15-0460 GBM patient-derived cells (n = 6, Mann-Whitney U test). **D-G.** qPCR expression of *SLIT1* (**D**), *SLIT3* (**E**), *ROBO1* (**F**) and *ROBO2* (**G**) in N15-0460 cells after shRNA *SLIT2* silencing (n = 4, Mann-Whitney U test). **H.** shCTRL and shSLIT2 treated N15-0460 growth over 72 hours in complete medium (n = 3, multiple comparison linear regression). **I.** shCTRL and shSLIT2 treated N15-0460 cells response to TMZ treatment (n = 4, Two-way ANOVA). **J.** Transwell assay quantification of N15-0460 cell migration towards a SLIT2 gradient (n = 4, Mann-Whitney U test). **K.** Transwell assay quantification of N15-0460 shCTRL or shSLIT2 cell migration towards a serum gradient (n = 4, Mann-Whitney U test). **L-M.** Spheroid formation assay quantification of shCTRL and shSLIT2 N15-0460 cells. Number (**L**) and size (**M**) of spheroids formed after 48 hours in culture were quantified (n = 6 cultures per group, Mann-Whitney U test). **N-O.** Quantification of spheroid invasion assay in fibrin gels of shCTRL and shSLIT2 N15-0460 cells after 24 (**N**) and 48 hours (**O**). Data are presented as mean ± s.e.m. * $P < 0.05$, ** $P < 0.01$, *** $P < 0.001$.

Supplemental Figure 4

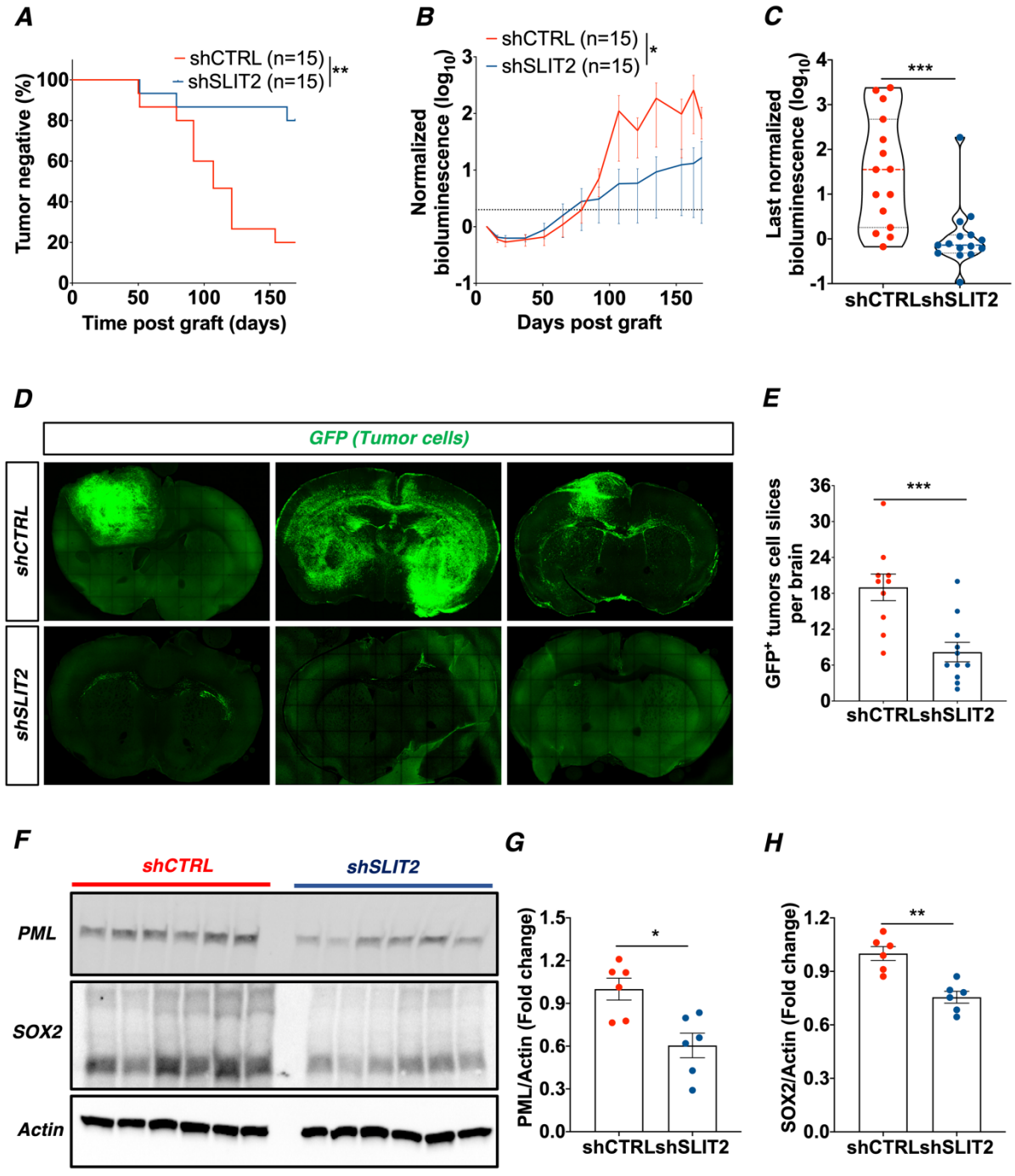

Supplemental Figure 4. *SLIT2* silencing slows tumor growth in a GBM Patient-derived Xenograft (PDX) model.

A. Tumor development curve after injection of shCTRL and shSLIT2 N15-0460 GBM patient-derived cells in nude mice (n = 15 mice per group, log-rank test). **B.**

bioluminescence signal over time after tumor injection (n = 15 mice per group, One-way ANOVA). **C.** bioluminescence signal at the end-point of experiment for each of the injected mice (n = 15 mice per group, Mann-Whitney U test). **D.** Tile-scan images of vibratome sections from implanted mice demonstrating GFP^+ tumor cell spread. **E.** Quantification of GFP^+ tumor cell spread (n = 10 shCTRL and 11 shSLIT2 mice, Mann-Whitney U test). **F-H.** Western blot analysis **(F)** and protein quantification of PML (**G**) and SOX2 (**H**) expression in shCTRL and shSLIT2 N15-0460 GBM cells (n = 6, Mann-Whitney U test, Actin blot is the same as in Supplemental Figure 3A). Data are presented as mean ± s.e.m. * $P < 0.05$, ** $P < 0.01$, *** $P < 0.001$.

Supplemental Figure 5

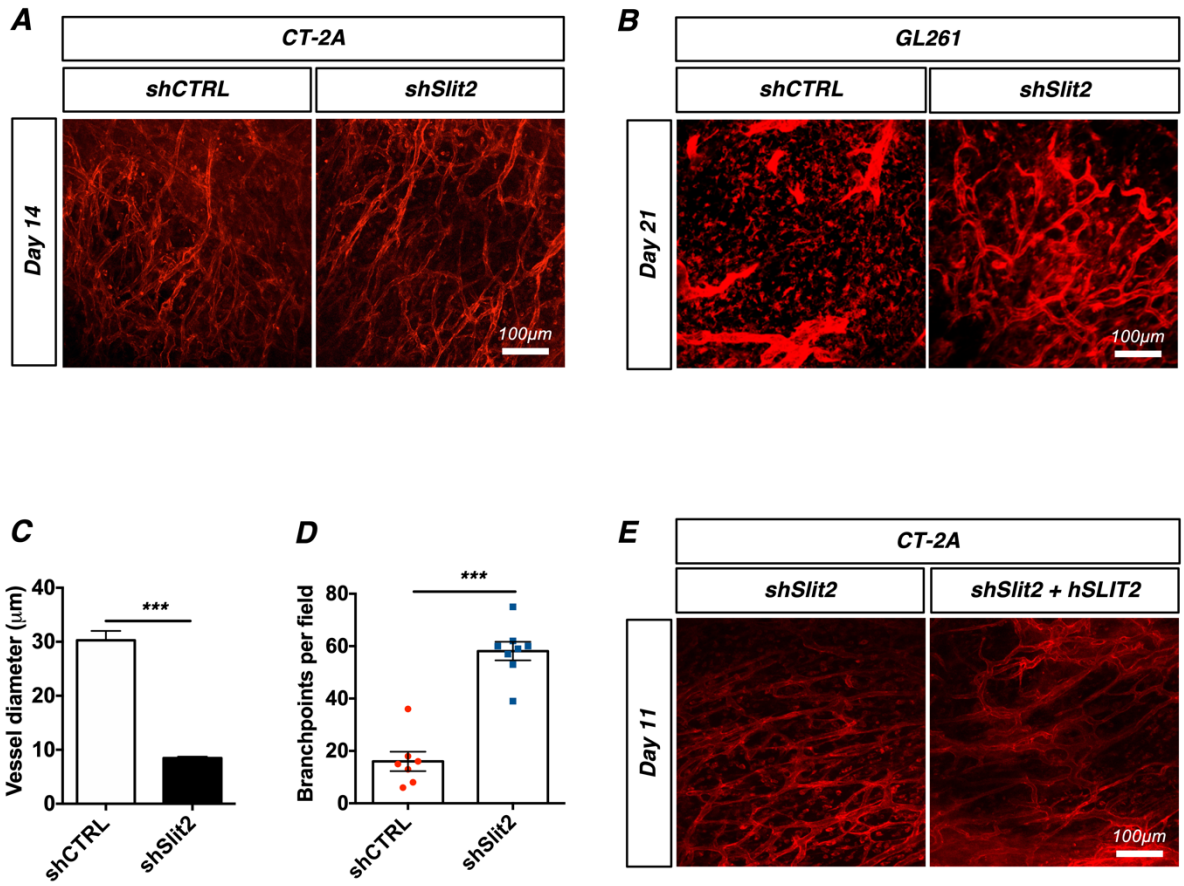

485

486 **Supplemental Figure 5. Slit2 drives vessel dysmorphia and vascular dysfunction in**

487 **CT-2A and GL261 glioma models.**

488 **A.** *In vivo* two-photon imaging of ROSA^{mTmG} mice bearing day 14 CT-2A shCTRL or

489 shSlit2 tumors. **B.** *In vivo* two-photon imaging of ROSA^{mTmG} mice bearing day 21 GL261

490 shCTRL or shSlit2 tumors. **C-D.** Quantification of blood vessel diameter (**C**) and

491 branchpoints (**D**) of the GL261 tumors shown in **(B)** (n = 7 mice per group, Student's t-

492 test). **E.** *In vivo* two-photon imaging of ROSA^{mTmG} mice bearing day 11 CT-2A shSlit2

493 or shSlit2+hSLIT2 tumors. Data are presented as mean ± s.e.m. * $P < 0.05$, ** $P < 0.01$,

494 *** $P < 0.001$

495

496

Supplemental Figure 6

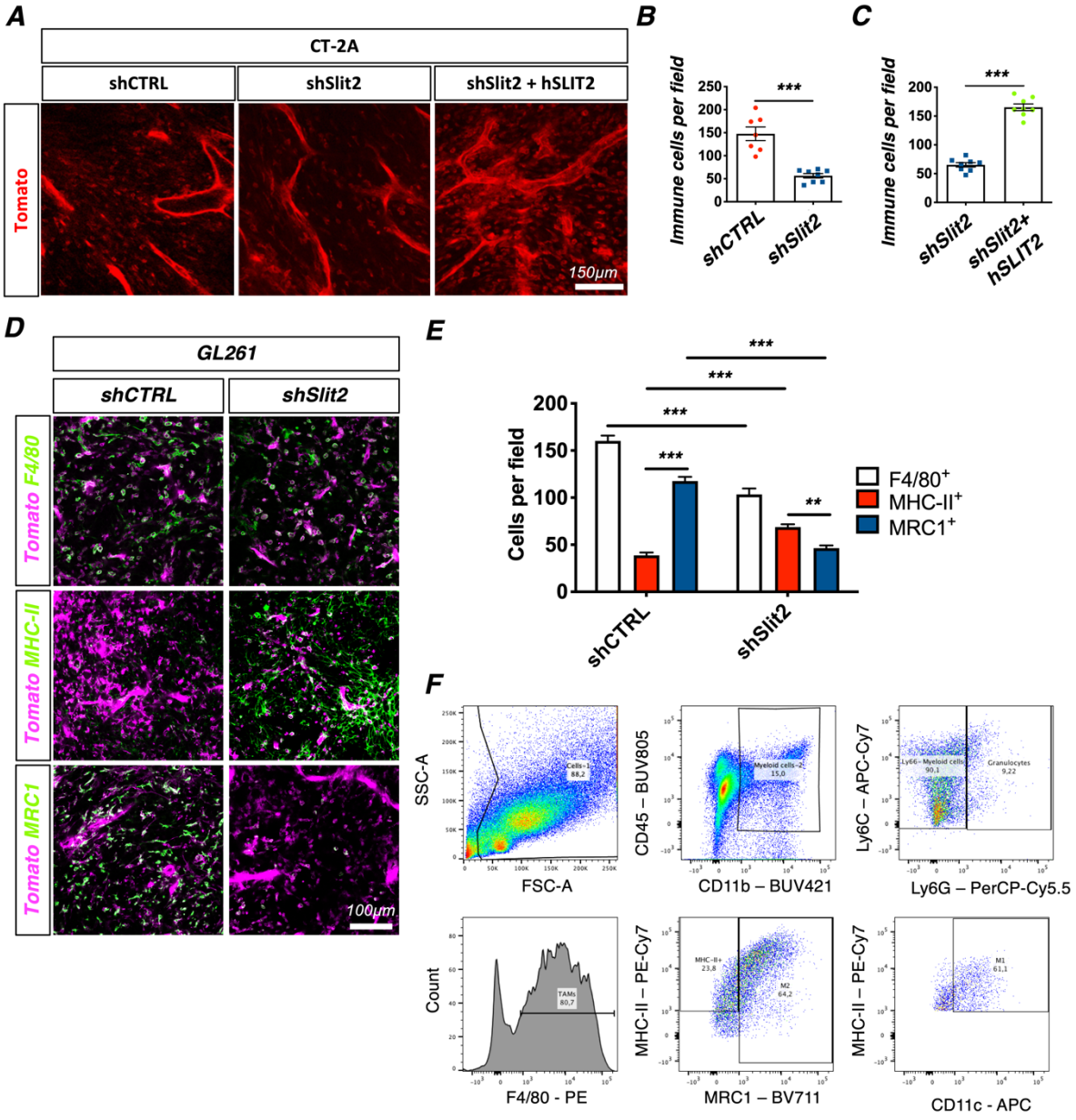

Supplemental Figure 6. Slit2 silencing favors macrophage cytotoxic polarization in CT-2A and GL261 glioma models.

A-C. *In vivo* imaging (**A**) and quantification (**B-C**) of host-derived tumor infiltrating immune cells (red) in late-stage CT-2A tumors (n = 7 shCTRL, n = 8 shSlit2 and shSlit2+hSLIT2 mice, Student's t-test). **D.** Immunohistochemistry on sections of day 21 GL261 shCTRL or shSlit2 tumors with antibodies recognizing F4/80, MHC-II and MRC1 (green). **E.** Quantifications of (**D**) (n = 7 mice per group, 5 fields per tumor, Two-Way ANOVA). **F**. Flow cytometry-gating strategy example for macrophage counting shown in **Figure 4C-E. G-H.** FACS quantification of Dendritic Cells (**G**, DCs, $CD45^+CD11b^+CD11c^+MHC\text{-}II^+F4/80^-$) and Neutrophils (**H**, $CD45^+CD11b^+Ly6G^+$). Data are presented as mean ± s.e.m. * $P < 0.05$, ** $P < 0.01$, *** $P < 0.001$.

Supplemental Figure 7

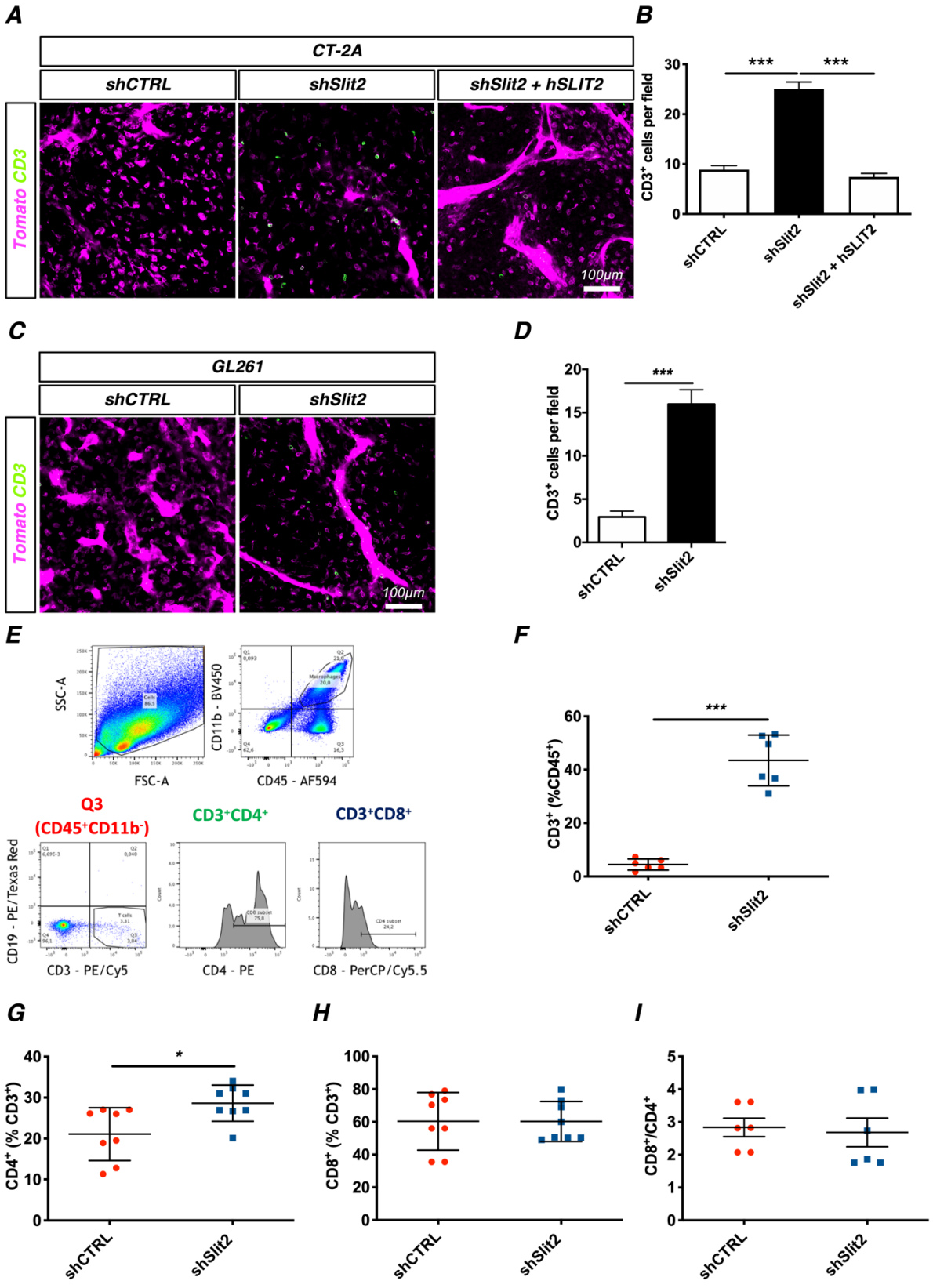

523

Supplemental Figure 7. Slit2 drives T cell depletion in CT-2A and GL261 models. **A.** Anti-CD3 staining (green) on sections of late stage CT-2A shCTRL, shSlit2 or shSlit2+hSLIT2 tumors. **B**. Quantification of (**A**) (n = 7 mice per group, 5 fields per tumor, One-Way ANOVA). **C**. Anti-CD3 staining (green) on sections of late stage GL261 shCTRL and shSlit2 tumors. **D**. Quantification of (**C**) (n = 7 mice per group, 5 fields per tumor, Student's t-test). **E-H**. Extension of flow-cytometry analysis from **Figure 5**. When considering only the immune cell compartment of the tumor microenvironment ($CD45^+$ cells), there is a 10-fold increase in the proportion of TALs (from 4.4% to 43.5%) in shSlit2 tumors **(F)**. Analysis of the percentage of $CD4^+$ T helper cells **(G)** and $CD8^+$ cytotoxic T cells **(H)** among the TALs (n = 8 mice per group, Mann-Whitney). **I.** Ratio between $CD8^+$ and $CD4^+$ TALS (n = 8 mice per group, Mann-Whitney). Data are presented as mean ± s.e.m. * $P < 0.05$, ** $P < 0.01$, *** $P < 0.001$.

Supplemental Figure 8

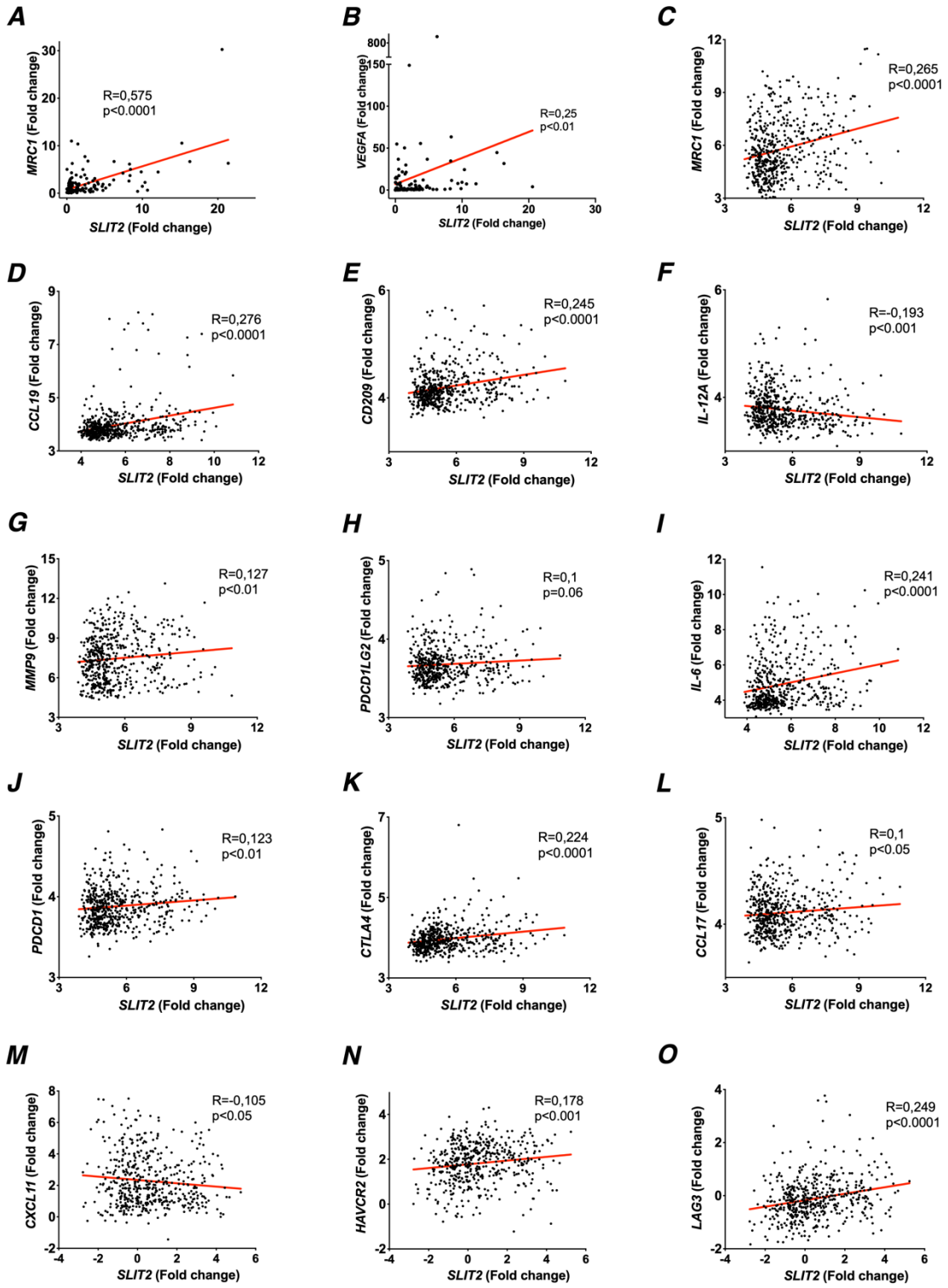

549

Supplemental Figure 8. SLIT2 expression correlated with immunosuppression in GBM patients.

A-B. Correlation analysis of *MRC1* (**A)** or *VEGFA* (**B**) and *SLIT2* expression in GBM patients (n = 129 patients, Spearman's correlation test). **C-O.** Correlation analysis of *SLIT2* expression with the indicated genes in GBM patients from TCGA cohort (n = 489 patients, Spearman's correlation test). * $P < 0.05$, ** $P < 0.01$, *** $P < 0.001$.

Supplemental Figure 9

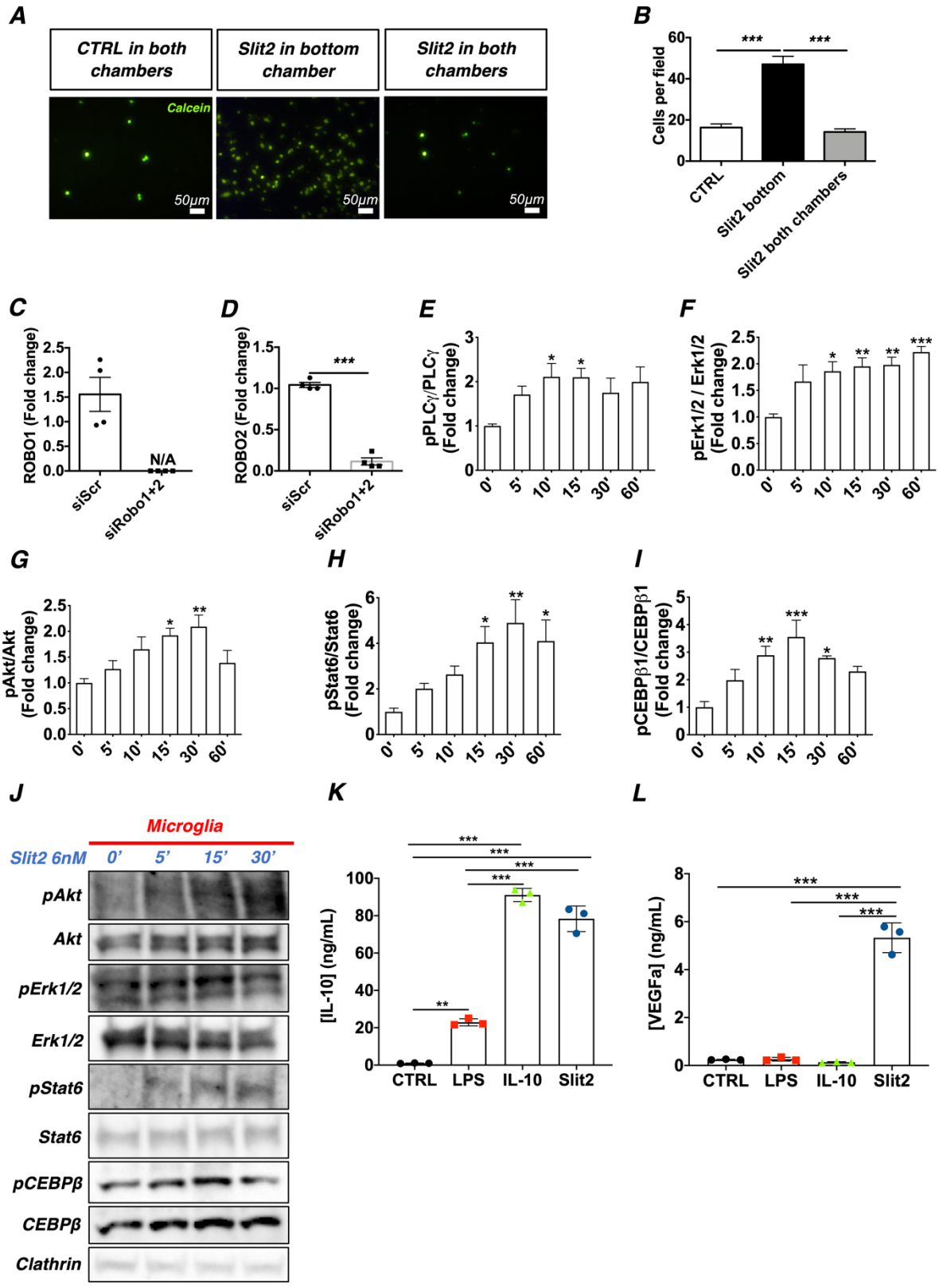

565

Supplemental Figure 9. Slit2 induces chemotactic migration and signaling in primary macrophages and microglial cells.

A-B. Representative images **(A)** of calcein-stained (green) Transwell assays with Slit2 treatment in the bottom chamber or in both chambers and quantification **(B)**. Slit2-induced migration is chemotactic, as treatment with Slit2 in both chambers disrupts the gradient and abrogates migration (n = 4, One-way ANOVA). **C-D.** qPCR analysis of Robo1 (**C**) and Robo2 (**D**) expression after siRNA treatment of cultured RAW264.7 macrophages for 72hs (n = 4, Mann Whitney). **E-I.** Quantifications of the Western Blots shown in **Figure 6F.** (n = 6, One-Way ANOVA). **J**. Western blot analysis of Slit2 downstream signaling in cultured microglial cells (n = 3). **K-L.** ELISA from conditioned medium from LPS or Slit2-treated microglial cells quantifying the secretion of IL-10 (**K**) and VEGFa (**L**) (n = 3 independent cultures, Mann-Whitney U test)**.** Data are presented as mean ± s.e.m. * $P < 0.05$, ** $P < 0.01$, *** $P < 0.001$.

Supplemental Figure 10

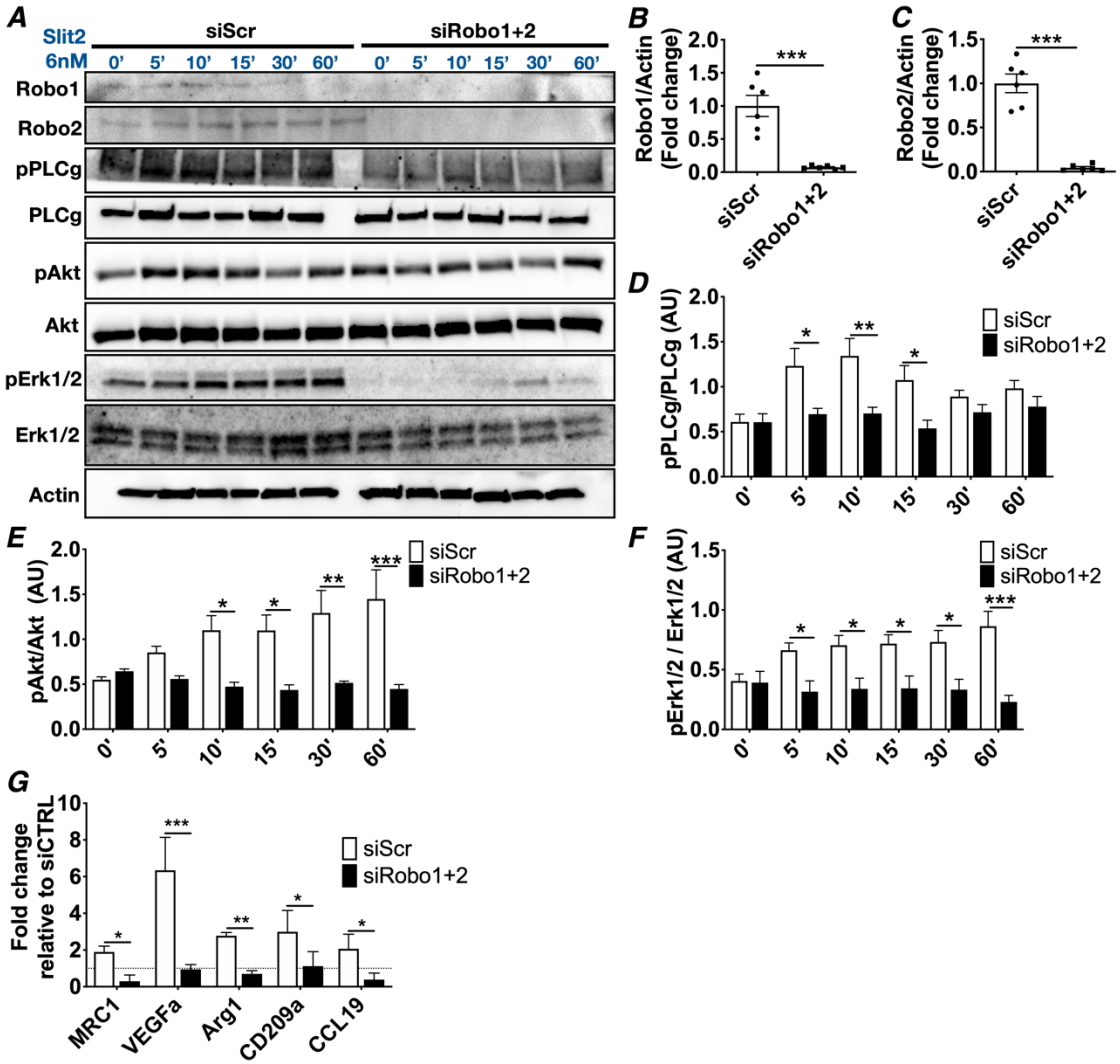

584 **Supplemental Figure 10. Slit2 induces macrophage migration and downstream**
585 **signaling via Robo1/2.**

586 **A.** Western blot analysis of PLCγ, Akt and Erk1/2 phosphorylation induced by Slit2 in
587 control and Robo1/2 knockdown RAW264.7 macrophages (n = 5). **B-C**. Quantification
588 of Robo1 (**A**) and Robo2 (**B**) protein expression after Robo1 and Robo2 knockdown. **D-**
589 **F**. Quantification of **(A)** (n = 5, Two-way ANOVA). **G.** qPCR analysis of genes related
590 to the tumor supportive phenotype (*Mrc1*, *Vegfa, Arg1, Cd209a* and *Ccl19*) in RAW264.7
591 macrophages after Robo1 and Robo2 knockdown and Slit2 treatment (n = 4, Mann
592 Whitney U test). Data are presented as mean ± s.e.m. * $P < 0.05$, ** $P < 0.01$, *** $P <$
593 0.001.

Supplemental Figure 11

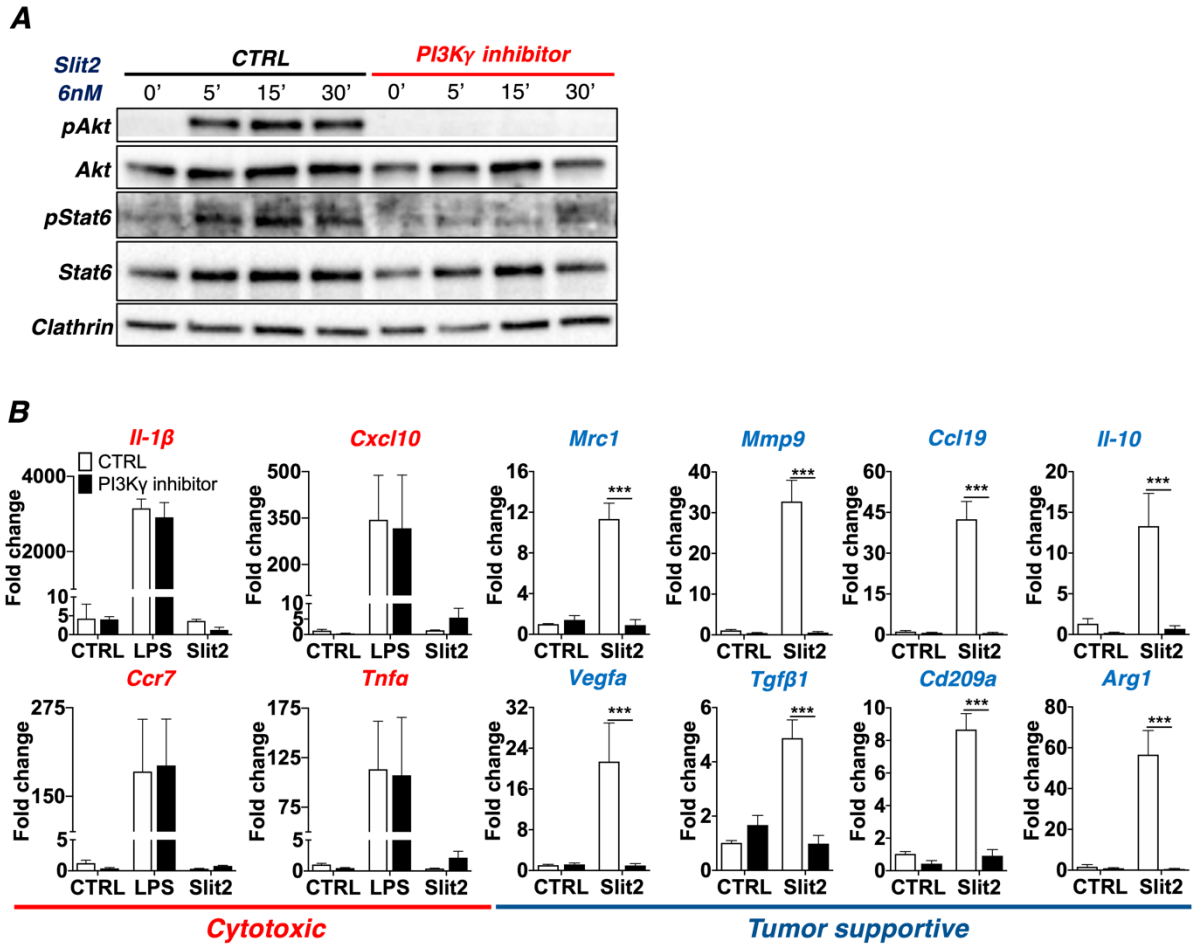

Supplemental Figure 11. PI3Kγ inhibiton disrupts Slit2-induced macrophage and microglia polarization.

A. WB analysis of Akt and Stat6 phosphorylation in BMDMs induced by Slit2 after PI3Kγ inhibitor IPI-549 pretreatment (n = 3 independent cultures). **B.** qPCR analysis of microglial cultures following Slit2 or LPS treatment after pre-treatment with PI3Kγ inhibitor (n = 4 independent cultures, 2-way ANOVA). Data are presented as mean ± s.e.m. * $P < 0.05$, ** $P < 0.01$, *** $P < 0.001$.

Supplemental Figure 12

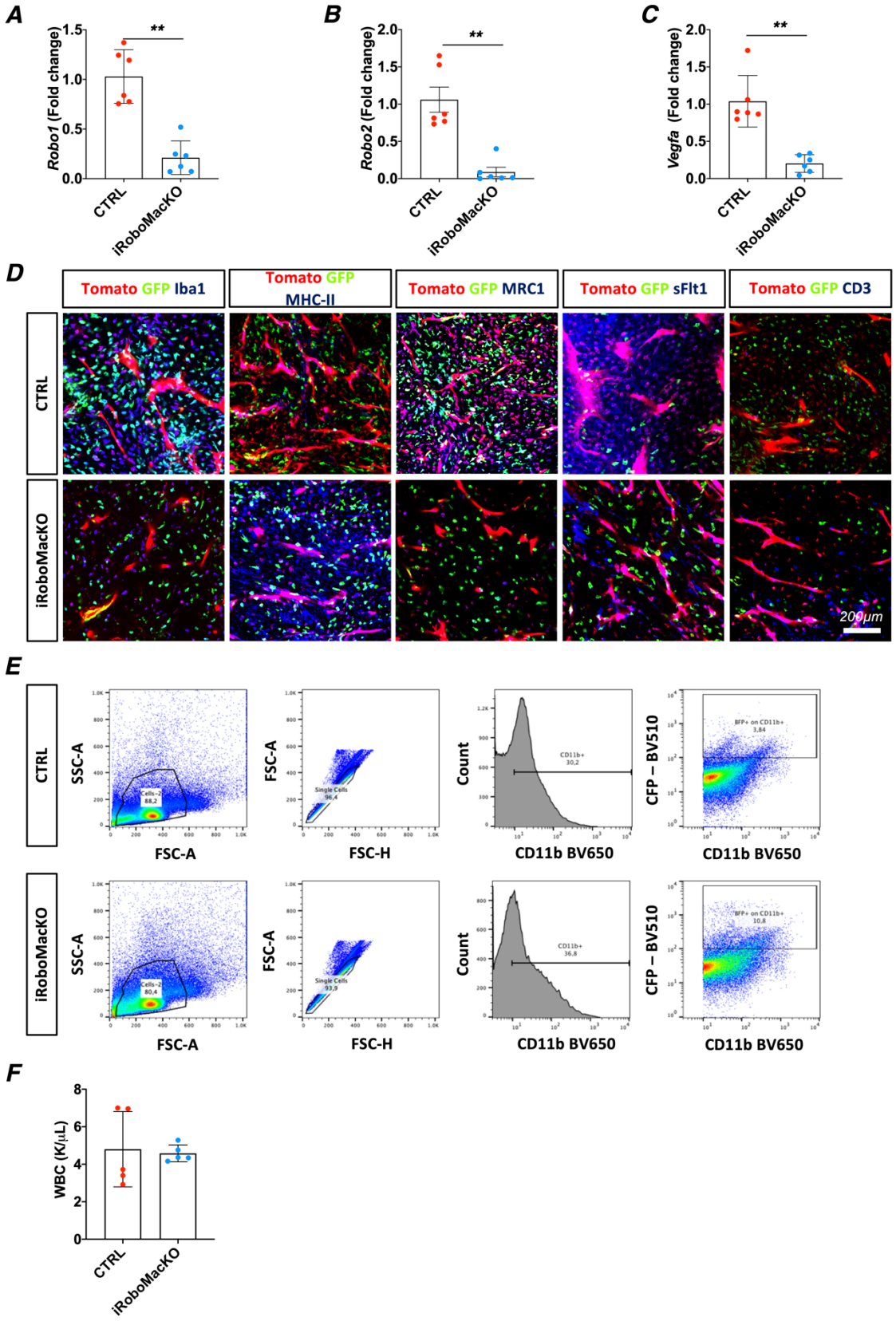

605

Supplemental Figure 12. Analysis of iRoboMacKO

A-C. qPCR of Robo1 (**A**), Robo2 (**B**) and Vegfa (**C**) in GFP^+ macrophages extracted from the bone-marrow of CTRL and iRoboMacKO tumor-bearing mice 21 days after tumor implantation. **D**. Immunohistochemistry images related to quantifications shown in **Figure 8I-K**. **E.** Flow cytometry-gating strategy example for graphs shown in **Figure 8M-N**. **F.** Total white blood cells (WBC) counts from peripheral blood of late-stage CTRL and iRoboMacKO tumor-bearing mice (n = 5 mice/group; Mann-Whitney U test). Data are presented as mean ± s.e.m. * $P < 0.05$, ** $P < 0.01$, *** $P < 0.001$.

Supplemental Figure 13

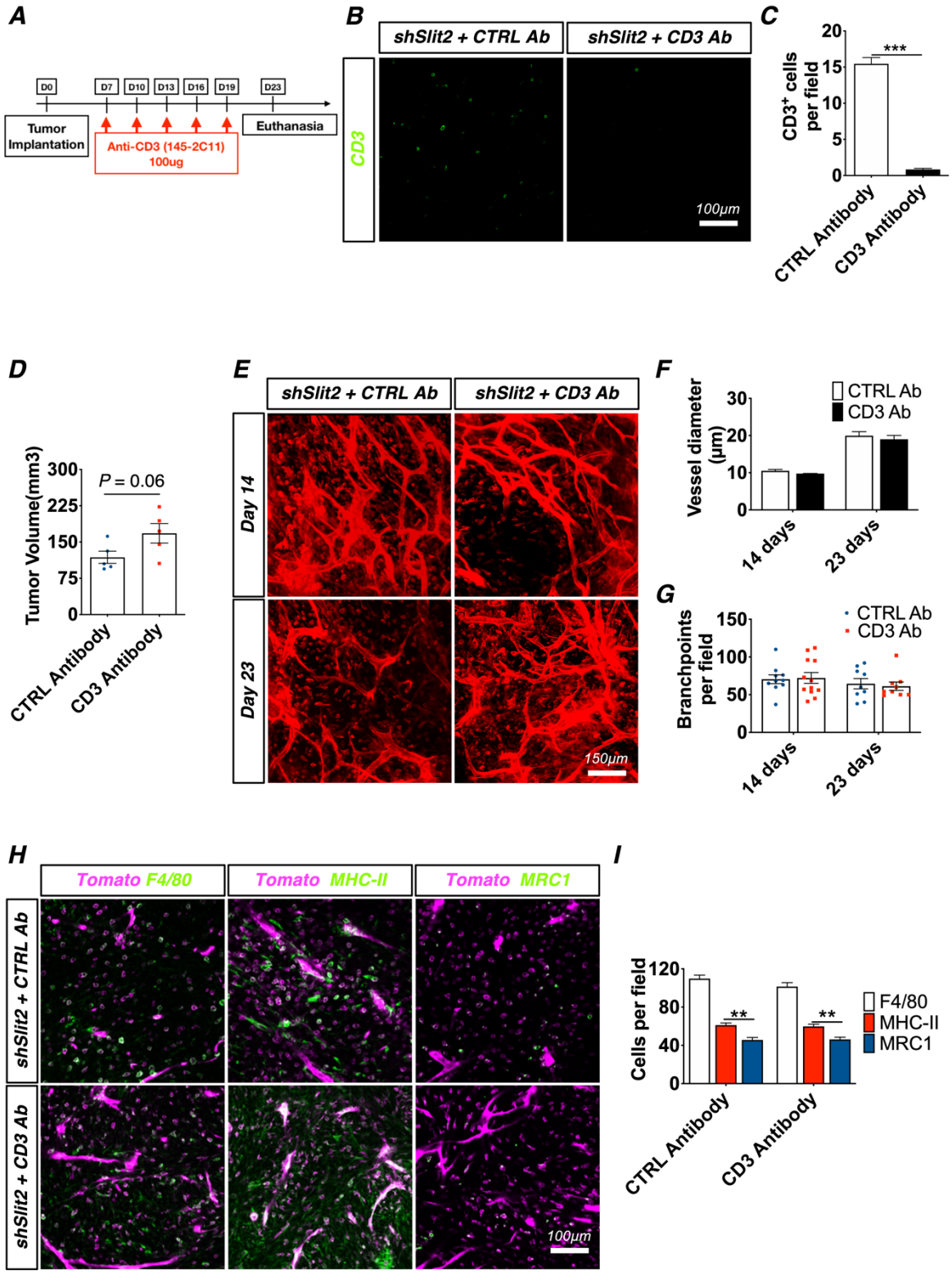

631

Supplemental Figure 13. *In vivo* T cell-depletion does not affect the TME.

A. Experimental design for T cell depletion by intravenous injection with 145-2C11 anti-CD3 antibodies (mice were treated with 100ug of 145-2C11 antibodies every 3 days starting 7 days after tumor implantation). **B.** CD3 immunostainings performed on sections of late stage CT-2A tumors. **C.** Quantification from **(B)** (n = 5 mice per group, 5 fields per staining, Student's t test). **D.** Tumor volume quantification at 23 days following anti-CD3 mAb treatment (n = 5 mice per group, Mann-Whitney U test). **E.** *In vivo* two-photon imaging of $ROSA^{mTmG}$ mice bearing early (14 days) and late stage (23 days) CT-2A shSlit2 tumors with or without anti-CD3 mAb treatment. **F-G.** Quantification of Blood vessel diameter **(F)** and branchpoints **(G)** from **€** (n = 5 mice per group, One-way ANOVA). **H.** F4/80, MHC-II and MRC1 Immunohistochemistry on sections of late stage (23 days) CT-2A shSlit2 tumors treated with control mAb or anti-CD3 mAb. **I.** Quantification from (**H**, n = 5 mice per group, 5 fields per tumor, Two-way ANOVA). Data are presented as mean ± s.e.m. * $P < 0.05$, ** $P < 0.01$, *** $P < 0.001$.

Supplemental Figure 14

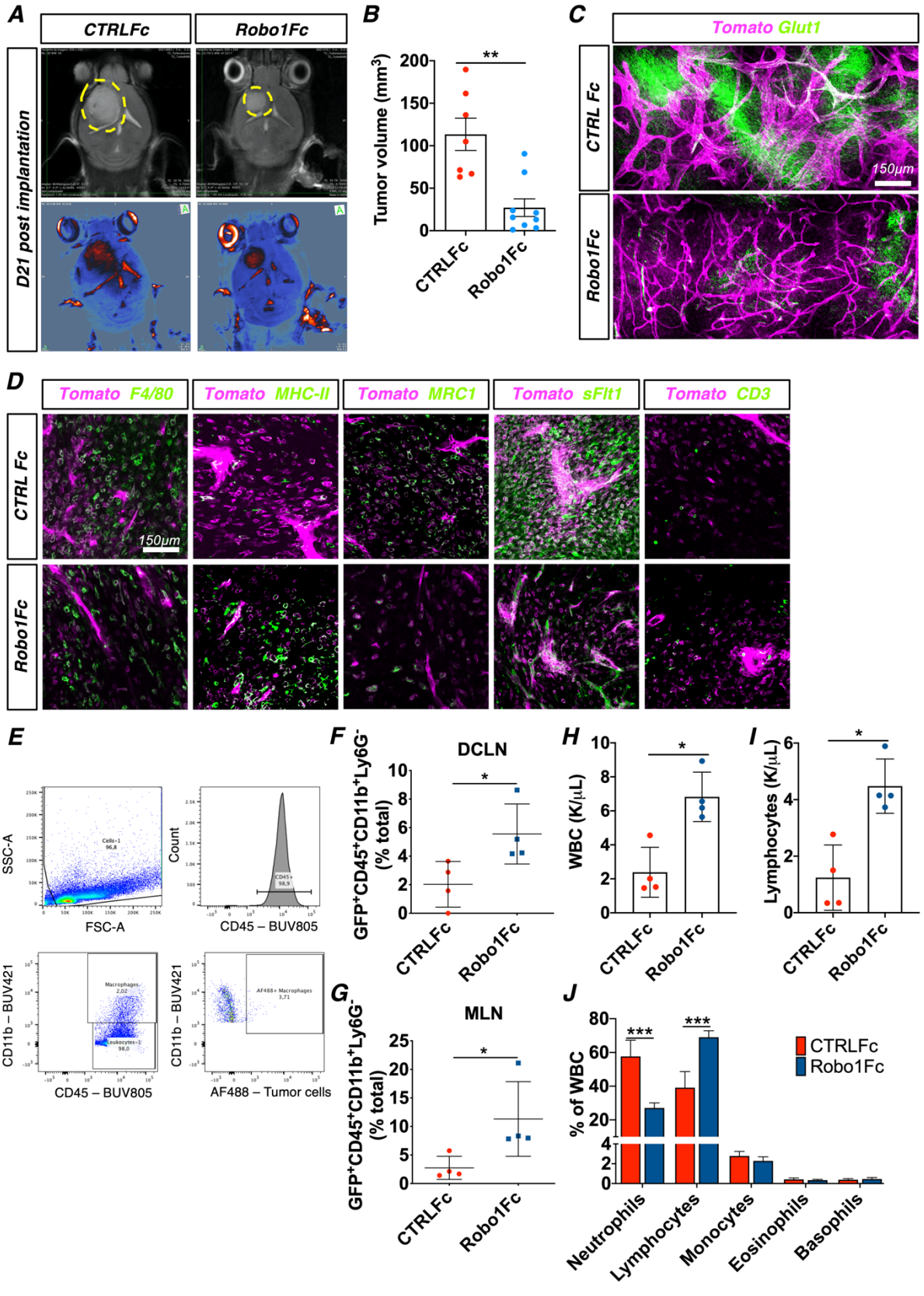

657

Supplemental Figure 14. Robo1Fc treatment slowed GBM growth by inducing systemic long-term anti-tumor immune responses.

A. T2-weighted post-gadolinium MRI images of CTRLFc and Robo1Fc treated mice 21 days after tumor implantation. **B.** Quantification of tumor size from (**A**) (n = 7 CTRLFc and 9 Robo1Fc tumors). **C.** Immuno-staining for Glut1 (quantified in **Figure 9H**). **D.** Immunohistochemistry images related to quantifications shown in **Figure 9I-K**. **E**. Flow cytometry-gating strategy example for graphs shown in (**F-G**). **F-G.** FACS analysis of deep cervical and mandibular lymph nodes (DCLN and MLN, respectively) from late-stage CTRLFc- and Robo1Fc-treated mice (n = 4 mice/group; Mann-Whitney U test). **H-J.** Total white blood (WBC, **H**), lymphocyte (**I)** and differential WBC (**J**) counts from peripheral blood of late-stage CTRLFc- and Robo1Fc-treated tumor-bearing mice (n = 4 mice/group; Mann-Whitney U test and Two-way ANOVA). Data are presented as mean ± s.e.m. * $P < 0.05$, ** $P < 0.01$, *** $P < 0.001$.

Primer	Cat No
HS_ROBO3_1_SG	QT00055951
Hs_ROBO2_2_SG	QT01007664
Hs_ROBO4_1_SG	QT00237741
Hs_SLIT2_1_SG	QT00007784
Hs_SLIT3_1_SG	QT00018795
Hs_SLIT1_1_SG	QT00071113
Hs_ROBO1_2_SG	QT01668982
Hs_ACTB_1_SG	QT00095431
Mm_ACTB_1_SG	QT00095242
Mm_GAPDH_3_SG	QT01658692
Mm_CCR7_1_SG	QT00240975
Mm_MRC1_1_SG	QT00103012
Mm_VEGFA_1_SG	QT00160769
Mm_CCL19_2_SG	QT02532173
Mm_TNF_1_SG	QT00104006
Mm_MMP9_1_SG	QT00108815
Mm_TGFB1_1_SG	QT00145250
Mm_IL1B_2_SG	QT01048355
Mm_PDCD1IG1_1_SG	QT00148617
Mm_PDCD1IG2_1_SG	QT00136640
Mm_CXCL10_1_SG	QT00093436
Mm_IL12B_1_SG	QT00153643
Mm_CD209A_1_SG	QT00116312
Mm_ARG1_1_SG	QT00134288
Mm_IL10_1_SG	QT00106169
Mm_IL12M_1_SG	QT00101108
Mm_IL2_1_SG	QT00112315
Mm_CXCL11_1_SG	QT00265041
Mm_IL17A_1_SG	QT00103278
Mm_IFNg_1_SG	QT01038821
Mm_CCL17_1_SG	QT00131572
Mm_PDCD1_1_SG	QT00111111
Mm_ROBO1_1_SG	QT00146853
Mm_SLIT1_1_SG	QT01044925
Mm_SLIT2_1_SG	QT00163828
Mm_SLIT3_1_SG	QT00283416
Mm_ROBO3_1_SG	QT00136605
Mm_ROBO2_1_SG	QT00143255

Supplemental Data Table. 1. List of qPCR Primers used in this study.